Materials Letters 130 (2014) 83–86

Contents lists available at ScienceDirect

Materials Letters

journal homepage: www.elsevier.com/locate/matlet

Facile synthesis and characterization of ultrathin MoS_2 nanosheets

Xianghua Zhang [a,b], Hua Tang [c], Maoquan Xue [c,d], Changsheng Li [a,c,*]

[a] School of Mechanical Engineering, Jiangsu University, Jiangsu Province,Zhenjiang 212013, China
[b] School of Mechanical Engineering, Jiangsu University of Technology, Jiangsu Province, Changzhou 213001, China
[c] School of Materials Science and Engineering, Jiangsu University, Jiangsu Province, Zhenjiang 212013, China
[d] Changzhou Institute of Light Industry Technology, Jiangsu Province, Changzhou 213164, China

ARTICLE INFO

Article history:
Received 13 March 2014
Accepted 14 May 2014
Available online 21 May 2014

Keywords:
MoS_2
Multilayer structure
Gas–solid reaction
Nanocrystalline materials

ABSTRACT

Ultrathin MoS_2 nanosheets with thickness of 5–10 nm were successfully synthesized by a facile gas–solid reaction method, using molybdenum trioxide (MoO_3) and thiourea as the precursors, and then calcined at 800–850 °C under N_2 for 1 h. As-prepared MoS_2 samples were characterized by XRD, EDS, FESEM, and TEM. TEM and FESEM results showed that the obtained MoS_2 ultrathin nanosheets mainly consisted of 5–10 layers stacking of the monatomic sheets. The influence of temperature on the formation of MoS_2 nanosheets was investigated. A possible two-step reaction mechanism is proposed to explain the formation of MoS_2 nanosheets on the basis of observations of a temperature-dependent morphology evolution process.

1. Introduction

During the past decades, MoS_2, as one member of inorganic transition metal sulfides, has elicited numerous studies because of its unique layered structure and related interesting functional properties. The layered structure consists of strong covalent bonding between Mo–S atomic but weak Van der Waals attraction between lattice layers [1,2]. This unique anisotropic layered structure result in excellent optical, electronic and mechanical properties and wide applications such as catalysts [3], lubricants [4], photoconductors [5], lithium ion battery anodes [6], and hydrogen storage [7].

To date, MoS_2 has been reported with different morphologies including nanotubes [8], fullerene-like nanoparticles [1,2], nanoplates [9,10], nanorods [11], nanoflowers [12], nanowires [13] and nanospheres [14]. Recently, ultrathin MoS_2 nanosheets have attracted considerable attention due to its extraordinary electrochemical properties. And various methods have been reported on the synthesis of ultrathin MoS_2 nanosheets, including scotch tape based micromechanical exfoliation [15], intercalation assisted exfoliation [16], liquid exfoliation [17], physical vapor deposition [18], and hydrothermal synthesis [19]. However, up to now, it is still desirable to develop a facile and scalable strategy to produce ultrathin MoS_2 nanosheets on a large scale in order to realize their practical applications.

Herein, ultrathin MoS_2 nanosheets with the thickness of 5–10 nm were successfully synthesized through a facile and reproducible gas–solid reaction approach using MoO_3 and thiourea as starting materials and the effect of temperature on the morphologies of the as-prepared MoS_2 samples was investigated. Furthermore, a possible formation mechanism for the MoS_2 nanosheets has been discussed in detail.

2. Experiment

Synthesis: Thiourea and MoO_3 were purchased from Sinopharm (Shanghai) Chemical Reagent Co., Ltd. All other reagents were of analytical grade and were used as received without further purification. In a typical synthesis, 0.4 g MoO_3 and 6.35 g thiourea were thoroughly ground for 15 min, and then the ground mixture was loaded in an alumina boat. This boat was quickly pushed into the hot zone of the tube furnace after the furnace temperature had stabilized at about 850 °C under the atmosphere of nitrogen. After calcination at 850 °C for 1 h, the tube furnace was allowed to cool down to room temperature, and 0.363 g black MoS_2 was collected. The yield of the MoS2 nanosheets is 81.7%.

Characterization: The X-ray diffraction (XRD) patterns were recorded using a D8 advance (Bruker-AXS) diffractometer with Cu Kα radiation (λ=0.1546 nm). The morphologies of the as-synthesized products were examined by field-emission scanning

* Corresponding author at: Jiangsu University, School of Materials Science and Engineering, 301 Xuefu Road, Zhenjiang, Jiangsu 212013, China. Tel./fax: +86 511 8879 0268.
E-mail address: changshengli2008@hotmail.com (C. Li).

http://dx.doi.org/10.1016/j.matlet.2014.05.078
0167-577X/

electron microscopy (FESEM, JEOL, JSM-7001F) and transmission electron microscopy (TEM, JEOL, JEM-2100).

3. Results and discussion

The crystallinity, structure, and phase purity of the prepared samples were confirmed by XRD and EDS. Fig. 1a shows the XRD pattern of the MoS_2 sample fabricated by the sulfurization of MoO_3 at 850 °C. All peaks in the XRD pattern can be readily indexed to the pure hexagonal (P63/mmc space group) MoS_2 phase, with lattice constants $a=3.16$ Å and $c=12.294$ Å, which are in good agreement with the reported values (JCPDS card no. 65-1951). No extra peaks are observed in the XRD pattern, indicating the high purity of the MoS_2 samples. The high background intensities of the XRD patterns may suggest the existence of amorphous materials in MoS_2 [20]. An energy-dispersive X-ray spectrometer (EDS) result as shown in Fig. 1b reveals that the sample consisted of element

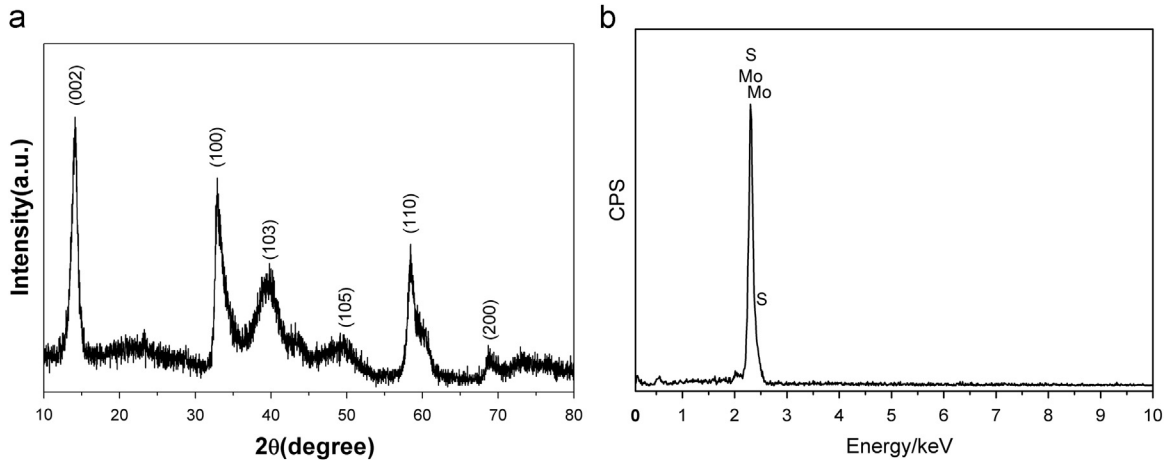

Fig. 1. (a) XRD pattern and (b) EDS of the as-prepared MoS_2 nanosheets.

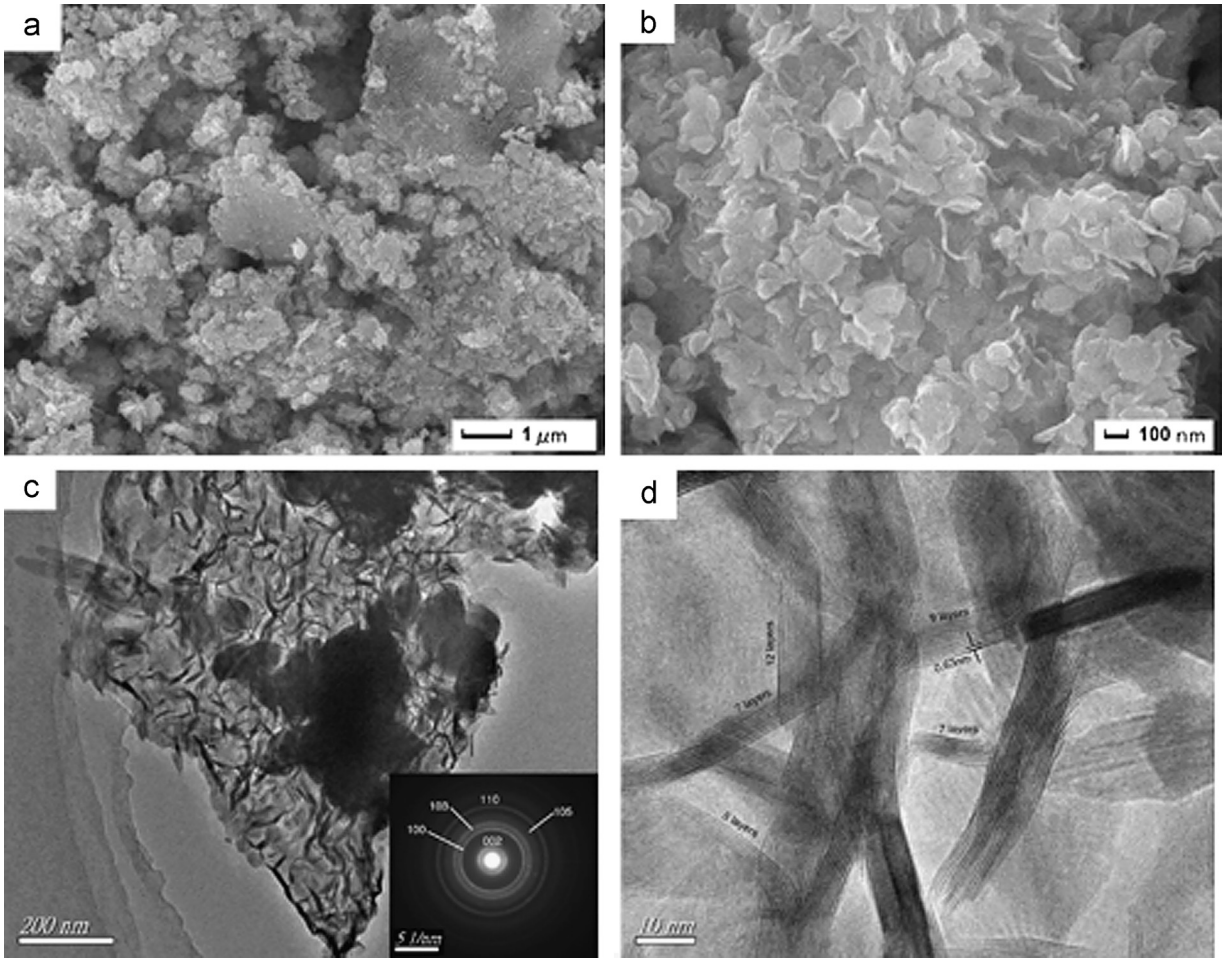

Fig. 2. FESEM (a, b) and TEM (c, d) of the MoS_2 nanosheets obtained at 850 °C for 1 h.

Mo and S, no another element is observed. Furthermore, the quantification of the peaks shows that the atom ratio between Mo and S is about 1:1.96, which is very close to the stoichiometric MoS_2.

The morphology of the obtained MoS_2 products was investigated by FESEM (Fig. 2a and b) and TEM (Fig. 2c and d). As can be seen from Fig. 2a, the product was composed of many aggregated particles. Fig. 2b, the high-magnification FESEM image, presents a clear view of the morphology. It reveals that the obtained samples mainly comprised of nanosheets, which have an average lateral size of about 100 nm and a thickness of 5–10 nm.

Further insight into the morphology and microstructure of MoS_2 nanoflakes was gained by TEM. As shown in Fig. 2(c), the low-magnification TEM image discloses that the as-synthesized MoS_2 particles comprised of well-dispersed sheets. The TEM image is in good agreement with the morphology as presented in the SEM pictures. The selected area electron diffraction (SAED) pattern for the MoS_2 nanosheets is presented in the inset of Fig. 2c. The diffraction rings can be indexed to the reflections of the molybdenum sulfide (002), (100), (103), (105) and (110) planes. The high-magnification TEM image, as shown in Fig. 2d, indicates that MoS_2 nanosheets mainly consisted of 5–10 layers stacking of the monatomic sheets. The interlayer separation between the MoS_2 layers is about 0.63 nm, which corresponds to the (002) plane of the MoS_2.

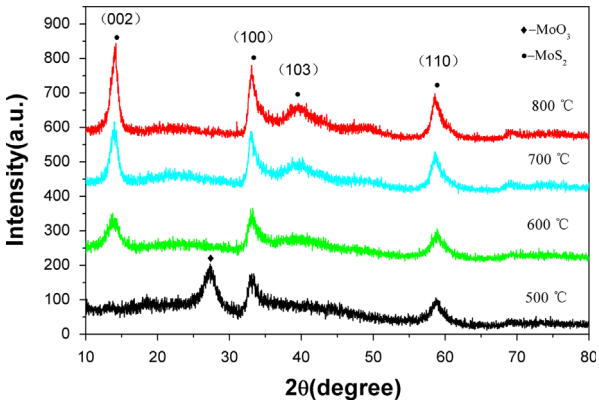

Fig. 3. XRD patterns of the samples obtained at different temperatures.

To better understand the formation mechanism of the MoS_2 nanolamellars, their growth process has been investigated by examining the samples harvested at different temperatures. Fig. 3 depicts the XRD patterns of the samples obtained at 500 °C, 600 °C, 700 °C and 800 °C, respectively. As shown in the figure, three lower intensities peaks can be detected after calcination at 500 °C for 1 h. And the most intensity peak among them, which are located in 2θ scale at 26°, is indexed to the (011) peak of MoO_3. The other two peaks located at 33.5° and 58.7° are corresponding to the (100) and (110) peak of MoS_2. This indicated that part of MoO_3 transformed into MoS_2 at 500 °C. The FESEM image of the sample harvested at 500 °C is presented in Fig. 4a. It is observed that the particles are evidently agglomerated. With the increase of reaction temperature to 600 °C, the (011) diffraction of MoO_3 disappeared and the (002) peak of MoS_2 appeared, which implies that MoO_3 has been completely sulfurized into MoS_2 at 600 °C. But the presence of broad and weak peaks indicates that MoS_2 particles have a very small crystallite size [21]. When the

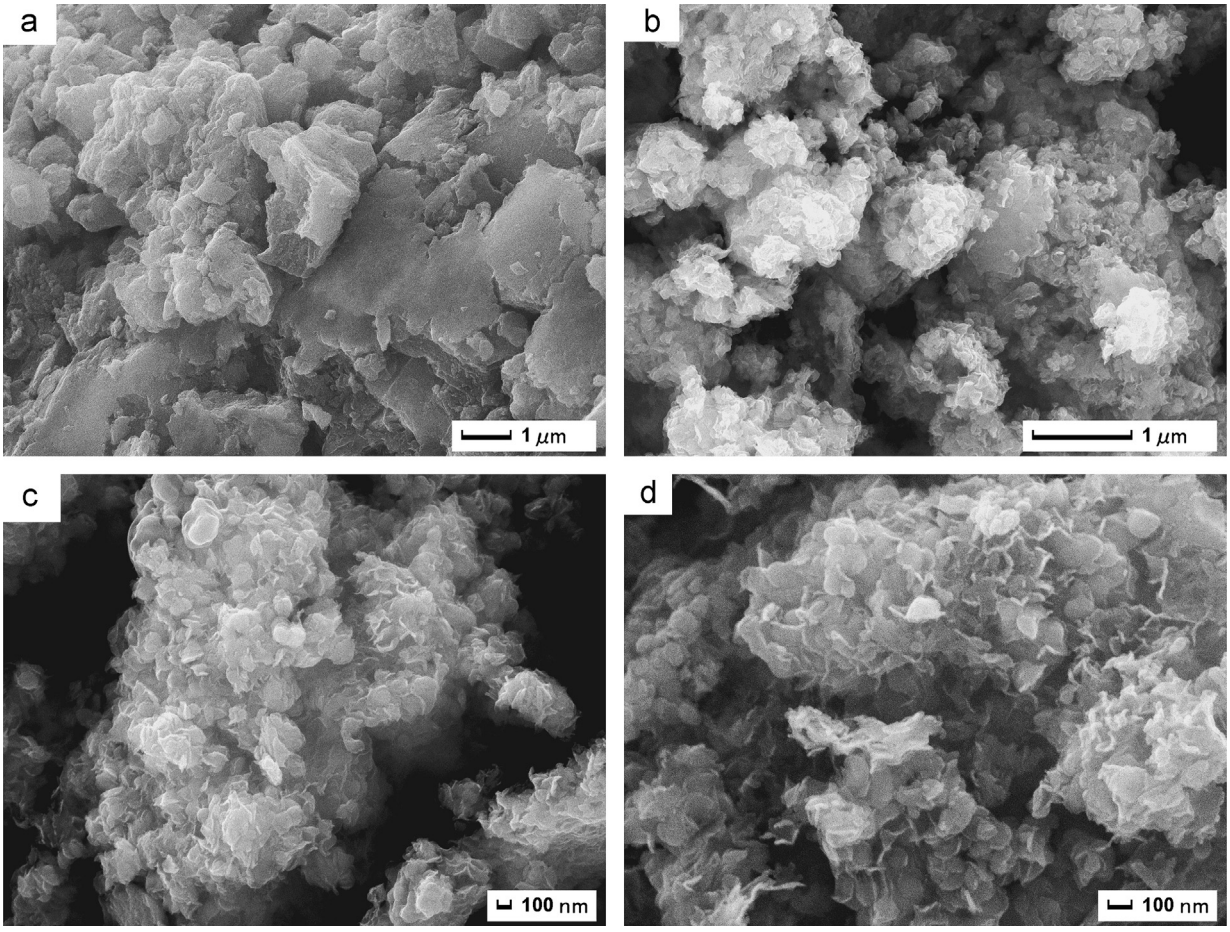

Fig. 4. SEM image of the MoS_2 nanosheets obtained at (a) 500 °C, (b) 600 °C, (c) 700 °C and (d) 800 °C.

reaction temperature is further increased to 700 °C and 800 °C, the intensity of the detected diffraction increased obviously. Moreover, it is obvious that the diffraction peaks of crystal plane (002) become stronger and sharper with increasing reaction temperature, suggesting the increase of the MoS_2 crystal sizes.

The FESEM images of the corresponding samples obtained at 600 °C, 700 °C and 800 °C are shown in Figs. 4b–d, respectively. From Fig. 4(b), it could be found that the sample obtained at 600 °C was mainly composed of aggregated particles, which is consisted of ultra-small nanosheets. However, when the heat-treatment temperature is raised to be higher than 600 °C, the lateral size of the nanosheets becomes bigger and the crystal morphology becomes clearer with the increase of annealing temperature.

Based on the above experimental results and the reported strategies in the synthesis of MoS_2 in literatures [1,2], especially the solid phase reaction of MoO_3 with S, we deduce that the formation of MoS_2 in this work go through a two-step reaction. In our strategy, thiourea instead of sulfur or H_2S served as the reductant and sulfurization agent at the same time. According to the literatures [22] reported, thiourea rapidly decomposed at high temperature and produced of CS_2, H_2NCN, and NH_3. Subsequently, CS_2 reduced Mo (VI) to Mo(IV), leading to the formation of MoS_2. At 850 °C, the reaction velocity of MoO_3 and CS_2 was very fast and layer-like MoS_2 structures immediately deposited on the surface of MoO_3 particles. With prolonging reaction time, the MoS_2 layers were exfoliated by the impact erosion of gases and further grown, which leading to the formation of the MoS_2 nanosheets. The detail growth process is shown in the Supporting information. The reaction routes for the synthesis of MoS_2 in our experiment could be expressed as follows:

$$2SC(NH_2)_2 \rightarrow CS_2 + H_2NCN + 2NH_3 \quad (1)$$

$$3CS_2 + 2MoO_3 \rightarrow 2MoS_2 + 3CO_2 + 2S \quad (2)$$

4. Conclusion

In summary, a facile route for fabricating ultrathin MoS_2 nanosheets was presented by the reaction of MoO_3 and thiourea in a nitrogen atmosphere at temperature of 800–850 °C for 1 h. Ultranthin MoS_2 nanosheets with thickness 5–10 nm and lateral size of about 100 nm were successfully synthesized through a two-step reaction including thiourea decomposition and MoO_3 sulfurization. The experimental results suggest that temperature plays a crucial role in the formation of MoS_2 nanosheets. The approach presented here can be extended to synthesize other metal sulfides nanomaterial.

Acknowledgments

This work was financially supported by National Natural Science Foundation of China (51275213, and 51302112), the Jiangsu National Nature Science Foundation (BK2011534, and BK2011480) and the Jiangsu Industry-University-Research Joint Innovation Foundation (BY213065-05, and BY213065-06).

Appendix A. Supporting information

Supplementary data associated with this article can be found in the online version at http://dx.doi.org/10.1016/j.matlet.2014.05.078.

References

[1] Tenne R. Angew Chem Int Ed 2003;42:5124–32.
[2] Tenne R. Nat Nanotechnol 2006;1:103–11.
[3] Chianelli RR, Berhault G, Torres B. Catal Today 2009;147:275–86.
[4] Chhowalla M, Amaratunga GAJ. Nature 2000;407:164–7.
[5] Ballif C, Regula M, Schmid PE, Remskar M, Sanjines R, Levy F. Appl Phys A 1996;62:543–7.
[6] Du GD, Guo ZP, Wang SQ, Zeng R, Chen ZX, Liu HK. Chem Commun 2010;46:1106–8.
[7] Rothschild A, Cohen SR, Tenne R. Appl Phys Lett 1999;75:4025–31.
[8] Chen J, Li SL, Xu Q, Tanaka K. Chem Commun 2002;16:1722–3.
[9] Wu ZZ, Wang DZ, Sun AK. J Cryst Growth 2010;312:340–3.
[10] Wu ZZ, Wang DZ, Liang X, Sun AK. J Cryst Growth 2010;312:1973–6.
[11] Albiter MA, Huirache-Acuna R, Paraguay-Delgado F, Rico JL, Alonso-Nunez G. Nanotechnology 2006;17:3473–81.
[12] Tang GG, Sun JR, Chen W, Wu KQ, Ji XR, Liu SS, et al. Mater Lett 2012;86:9–12.
[13] Li WJ, Shi EW, Ko JM. J Cryst Growth 2003;250:418–22.
[14] Ma L, Xu LM, Xu XY, Luo YL, Chen WX. Mater Lett 2009;63:2022–4.
[15] Radisavljevic B, Radenovic A, Brivio J, Giacometti V, Kis A. Nat Nanotechnol 2011;6:147–50.
[16] Zeng Z, Yin Z, Huang X, Li H, He Q, Lu G, et al. Angew Chem Int Ed 2011;50:11093–7.
[17] Zhou KG, Mao NN, Wang HX, Peng Y, Zhang HL. Angew Chem Int Ed 2011;50:10839–42.
[18] Lauritsen JV, Kibsgaard J, Helveg S, Topsoe H, Clausen BS, Lagsgaard E, et al. Nat Nanotechnol 2007;2:53–8.
[19] Altavilla C, Sarno M, Ciambelli P. Chem Mater 2011;23:3879–85.
[20] Zhang YC, Li J, Zhang M, Dionysios D. Environ Sci Technol 2011;45:9324–31.
[21] Gu F, Wang SF, Lu MK, Zhou GJ, Xu D, Yuan DR. J Phys Chem B 2004;108:8119–23.
[22] Wang S, Gao QY, Wang JC. J Phys Chem B 2005;109:17281–9.